IEEE Access
Multidisciplinary : Rapid Review : Open Access Journal

Received May 11, 2019, accepted May 27, 2019, date of publication May 30, 2019, date of current version June 11, 2019.

Digital Object Identifier 10.1109/ACCESS.2019.2920064

A Strategy Using Variational Mode Decomposition, L-Kurtosis and Minimum Entropy Deconvolution to Detect Mechanical Faults

HUI LIU AND JIAWEI XIANG
Laboratory of Structural Dynamics, Monitoring and Fault Diagnosis, College of Mechanical and Electrical Engineering, Wenzhou University, Wenzhou 325035, China

Corresponding author: Jiawei Xiang (jwxiang@wzu.edu.cn)

This work was supported by the National Science Foundation of China under Grant U1709208 and Grant 51575400.

ABSTRACT When faults occur in mechanical components, the faulty information is usually manifested as a series of periodic impulses which correspond to the faulty feature frequencies. However, due to the non-stationary characteristic of the raw vibration signals, the faulty feature frequencies are difficult extracted. In this paper, a novel strategy using variational mode decomposition (VMD), L-Kurtosis and minimum entropy deconvolution (MED) is proposed to detect mechanical faults. First, VMD is employed to decompose the raw vibration signal into a set of intrinsic mode functions (IMFs) to eliminate the interference of the noise. Second, the optimal intrinsic mode function (IMF) which contains the faulty information is determined using L-Kurtosis. Then, the impact characteristic of the periodic impulses in optimal IMF is enhanced through MED. Finally, a Hilbert envelope spectrum analysis is performed to the enhanced signal to extract the faulty feature frequency. In order to illustrate the performance of the proposed strategy, the simulation signal and real experimental signals collected from faulty rolling element bearings and gears are analyzed. The results show that the strategy using the VMD, L-Kurtosis, and MED can detect mechanical component faults effectively.

INDEX TERMS Variational mode decomposition, L-Kurtosis, minimum entropy deconvolution, rotary mechanical component, fault detection.

I. INTRODUCTION

As the rotary components widely used in modern machinery, rolling element bearing and gear play an increasingly important role. Once faults occur in bearing and gear, may lead to the direct economic losses and heavy casualties [1]. Therefore, it is of particular importance to exactly detect the faults in bearings and gears.

In the field of fault diagnosis and condition monitoring, vibration analysis has been proved to be the most commonly used and effective technique [2], [3]. For bearing and gear, the faulty information is usually manifested as a series of periodic impulses which correspond to the faulty feature frequencies [4], [5]. However, due to the interference of the environmental noise and other vibration sources, the faulty feature frequencies are difficult to be extracted.

With the rapid development of fault diagnosis techniques, plenty of signal processing methods have been proposed, which can be divided into three categories, i.e., the time domain methods, frequency domain methods and time-frequency domain methods. Due to the strong time and frequency localization ability [6], [7], the time-frequency domain methods, such as empirical modes decomposition (EMD) [8], local mean decomposition (LMD) [9]–[12], intrinsic time-scale decomposition (ITD) [13], [14] etc. have been widely applied in academic and engineering areas. Among them, EMD is suitable to analyze the non-stationary vibration signal. However, EMD has its intrinsic drawbacks, i.e., the mode mixing phenomena and unreliable theoretical basis. Similar to EMD, there are also insurmountable drawbacks in LMD and ITD, such as signal mutation, end effects and signal distortion etc. Compared with the above methods, variational mode decomposition (VMD) [15] not only has good adaptive signal decomposition performance, but also has solid theoretical basis. Each intrinsic mode function (IMF) decomposed by VMD preserves the natural oscillatory mode of the raw vibration signal [16]. Abdoos et al. verified that VMD can effectively extract the faulty features from

The associate editor coordinating the review of this manuscript and approving it for publication was Chuan Li.

vibration signals, and its performance in separation and noise robustness were confirmed in [17]–[22].

However, how to select the optimal IMF which contains the faulty information is a very knotty problem. As a widely used indicator, kurtosis [23] achieves good results in vibration analysis [24], [25]. However, the performance of kurtosis is greatly limited by its intrinsic drawback which makes it very susceptible to the outliers. Compared to kurtosis, L-Kurtosis [26] gives good impulse recognition performance while overcoming the drawback of kurtosis. For faulty bearing and gear, the IMF corresponding to the maximum L-Kurtosis value might be the optimal signal which contains the faulty information.

The minimum entropy deconvolution (MED) technique [27] was first proposed by Ralph Wiggins, which can enhance the periodic impulses through deconvolving the effect of the transmission path. The technique was originally used to identify and locate layers of subterranean minerals. After that, Endo and Randall [28] applied MED to detect faults in gear from the significantly enhanced impulses. Therefore, MED may be a powerful tool to detect faults in rotary components.

Based on the above, the combination of VMD, L-Kurtosis and MED might be an effective fault detection strategy, and the rest of this paper is structured as follows. Section II is divided into three parts which give the representations of the theoretical backgrounds of VMD, L-Kurtosis and MED, respectively. Section III describes the proposed strategy. In Section IV, verification of the proposed method is performed using the simulated data and the experimental data collected from faulty bearings and gears. Finally, the conclusions are drawn in Section V.

II. THEORETICAL BACKGROUND

A. VARIATIONAL MODE DECOMPOSITION

As a widely used time-frequency analysis method, VMD has good performance in signal decomposition. For the non-stationary signals $y(t)$, it can be decomposed into a set of IMFs u_k as [15]:

$$y(t) = \sum\nolimits_k u_k \tag{1}$$

The essence of VMD is to solve the optimal solution of constrained variational model by:

$$\min_{\{u_k\}\{\omega_k\}} \left\{ \sum\nolimits_k \left\| \partial_t \left[\left(\delta(t) + \frac{j}{\pi t} \right) * u_k(t) \right] e^{-j\omega_k t} \right\|_2^2 \right\} \tag{2}$$

where $\{u_k\} = \{u_1, \ldots, u_k\}$ is the set of decomposed IMFs, $\{\omega_k\} = \{\omega_1, \ldots, \omega_k\}$ is the set which contains the center frequency corresponding to each decomposed IMF, $\|\bullet\|_2$, δ and $*$ are the Euclid norm, Dirac distribution and convolution operator, respectively.

Here, a quadratic penalty term α and Lagrangian multipliers $\lambda(t)$ are introduced to convert the constrained problem into unconstrained problem, and the unconstrained variational model can be given by:

$$\begin{aligned} &L(\{u_k\}, \{\omega_k\}, \lambda) \\ &= \alpha \sum_k \left\| \partial_t \left[\left(\delta(t) + \frac{j}{\pi t} \right) * u_k(t) \right] e^{-j\omega_k t} \right\|_2^2 \\ &\quad + \left\| y(t) - \sum_k u_k(t) \right\|_2^2 + \left\langle \lambda(t), y(t) - \sum_k u_k(t) \right\rangle \end{aligned} \tag{3}$$

The update equations of u_k, ω_k and $\lambda(t)$ can be defined as:

$$\hat{u}_k^{n+1}(\omega) = \frac{\hat{y}(\omega) - \sum_{i>k} \hat{u}_i(\omega) + \frac{\hat{\lambda}(\omega)}{2}}{1 + 2\alpha(\omega - \omega_k)^2} \tag{4}$$

$$\hat{\omega}_k^{n+1} = \frac{\int_0^\infty \omega \left| \hat{u}_k(\omega) \right|^2 \mathrm{d}\omega}{\int_0^\infty \left| \hat{u}_k(\omega) \right|^2 \mathrm{d}\omega} \tag{5}$$

$$\hat{\lambda}^{n+1}(\omega) = \hat{\lambda}^n(\omega) + \tau \left(\hat{y}(\omega) - \sum_k \hat{u}_k^{n+1}(\omega) \right) \tag{6}$$

in which the mark $\wedge$ represents the update value of u_k, ω_k, $\lambda(t)$ and y, τ is update parameter.

B. L-KURTOSIS

As an effective indicator used in fault detection, L-Kurtosis can give a more correct parameter estimates than kurtosis. In this paper, L-Kurtosis is introduced to select the optimal IMF which contains the faulty information [26].

Here, we suppose $u_1, \ldots, u_q$ is a continuous independent sample from a cumulative distribution $F(u)$ and $u_{1:q}, \ldots u_{q:q}$ is the corresponding order statistics, respectively. The rth L-moment η_r [26] can be defined as:

$$\eta_r = \frac{1}{r} \sum_{k=0}^{r-1} (-1)^r \binom{r-1}{k} E(u_{r-k:r}), \quad r = 1, 2, \ldots \tag{7}$$

$E(u_{r-k:r})$ is given by:

$$\begin{aligned} &E(u_{r-k:r}) \\ &= \frac{r!}{(r\text{-k} - 1)!k!} \int_0^1 u[F(u)]^{r-k-1}[1 - F(u)]^k dF(u) \end{aligned} \tag{8}$$

Therefore, the first four order L-moment can be described as

$$\eta_1 = EU = b_0 = \int_0^1 u dF(u) \tag{9}$$

$$\begin{aligned} \eta_2 &= \frac{1}{2} E(u_{2:2} - u_{1:2}) = 2b_1 - b_0 \\ &= \int_0^1 u(2F(u) - 1) dF(u) \end{aligned} \tag{10}$$

$$\begin{aligned} \eta_3 &= \frac{1}{3} E(u_{3:3} - 2u_{2:3} + u_{1:3}) = 6b_2 - 6b_1 + b_0 \\ &= \int_0^1 u\left(6F^2(u) - 6F(u) + 1\right) dF(u) \end{aligned} \tag{11}$$

$$\begin{aligned} \eta_4 &= \frac{1}{4} E(u_{4:4} - 3u_{3:4} + 3u_{2:4} - u_{1:4}) \\ &= 20b_3 - 30b_2 + 12b_1 - b_0 \\ &= \int_0^1 u\left(20F^3(u) - 30F^2(u) + 12F(u) - 1\right) dF(u) \end{aligned} \tag{12}$$

where $b_i = \int_0^1 uF(u)^i dF(u)$, $i = 0, 1, 2, 3$ is the ith order weighted moment ($i = 0, 1, 2, 3$).

The L-Kurtosis value can be calculated by

$$\begin{aligned} L-Kurtosis &= \frac{\eta_4}{\eta_2} = \frac{E(u_{4:4} - 3u_{3:4} + 3u_{2:4} - u_{1:4})}{2E(u_{2:2} - u_{1:2})} \\ &= \frac{E(u_{4:4}) - E(u_{1:4}) - 3[E(u_{3:4}) - E(u_{2:4})]}{2[E(u_{2:2}) - E(u_{1:2})]} \end{aligned} \quad (13)$$

C. MINIMUM ENTROPY DECONVOLUTION

The essence of MED is an inverse filter which can counteract the effect of the transmission path and its basic idea is shown in Fig.1. For the optimal IMF u_h, without any prior knowledge about the impulsive sources, the MED filter could adaptively adjust the filter coefficients by optimizing the objective function of the output $u_o(t)$. Generally, high order statistic (such as kurtosis, skewness, etc.) is often employed as an objective function to quantify the character of a signal. More details on how to perform the MED analysis can be found in [30], [31].

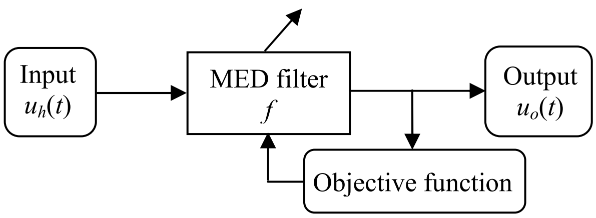

FIGURE 1. The basic idea of MED.

III. THE STRARTEGY USING VMD, L-KURTOSIS AND MED

In order to identify the faults of mechanical components (bearings and gears), a novel fault detection strategy using VMD, L-Kurtosis and MED is proposed. As described in Section II, VMD has the obvious advantage in decomposing the non-stationary signal. The introduction of L-Kurtosis not only solves the problem of how to select the optimal IMF but also effectively tracks the faulty information. MED can be employed to enhance the impact characteristic of periodic impulses, which provides great convenience for subsequent envelope analysis. Therefore, the combination of these three methods might be a robust strategy and the flowchart of the proposed strategy is given in Fig.2. The detailed procedure is summarized as follows:

Step1: Decompose the raw vibration signals using VMD.

VMD is employed to decompose the signals into a set of IMFs which contain the faulty information, and the interference of noise can be almost eliminated.

Step2: Select the optimal IMF using L-Kurtosis.

Aiming at the problem of how to select the optimal IMF, L-Kurtosis is introduced and the IMF corresponding to the maximum L-Kurtosis value is the optimal.

Step3: Enhance impact characteristic using MED.

In order to highlight the faulty feature frequencies, MED is further employed to enhance the impact characteristic of the optimal IMF.

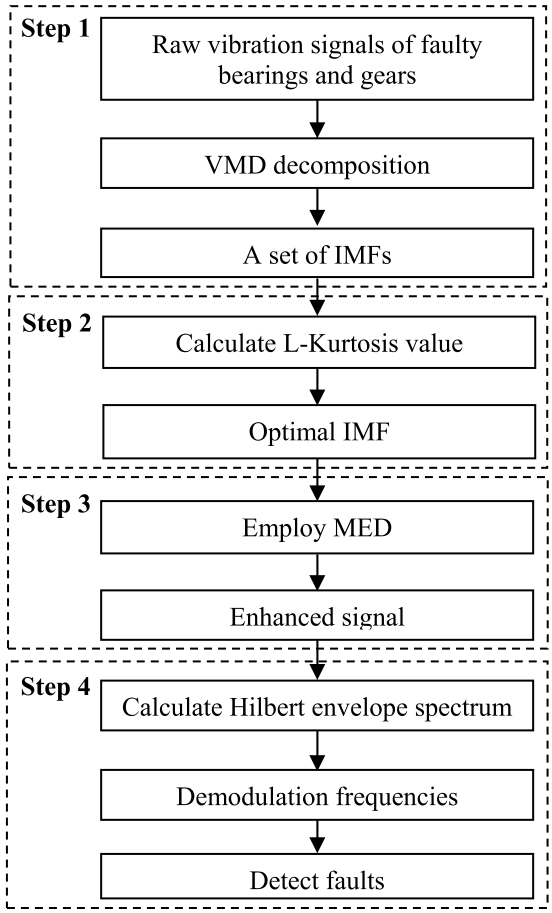

FIGURE 2. The flowchart of the proposed fault detection strategy.

Step4: Perform Hilbert envelope analysis and obtain the detect result.

A Hilbert envelope analysis is performed to the enhanced signal to extract the fault feature frequency. Through comparing the demodulation frequency with the theoretical feature value, the detection result is obtained.

IV. NUMERICAL SIMULATION

In this section, a numerical simulation is conducted to verify the performance of the proposed strategy. By the comparison investigation, it shows that the combination of the three methods is necessary and effective.

The simulation signal $y(t)$ is constructed as:

$$y(t) = x(t+T) + r(t) + n(t) \quad (14)$$

where $x(t)$ is the impulse, T is the impulse period, $r(t)$ is the interference signal (rotating frequency) and its harmonic components, $n(t)$ is the noise component.

In Eq.(14),$x(t)$ and $r(t)$ are:

$$x(t) = e^{-St}\cos(2\pi f_n t) \quad (15)$$

$$r(t) = P \times (5\sin(2\pi f_0 t) + 1.5\sin(4\pi f_0 t) + 0.5\sin(6\pi f_0 t)) \quad (16)$$

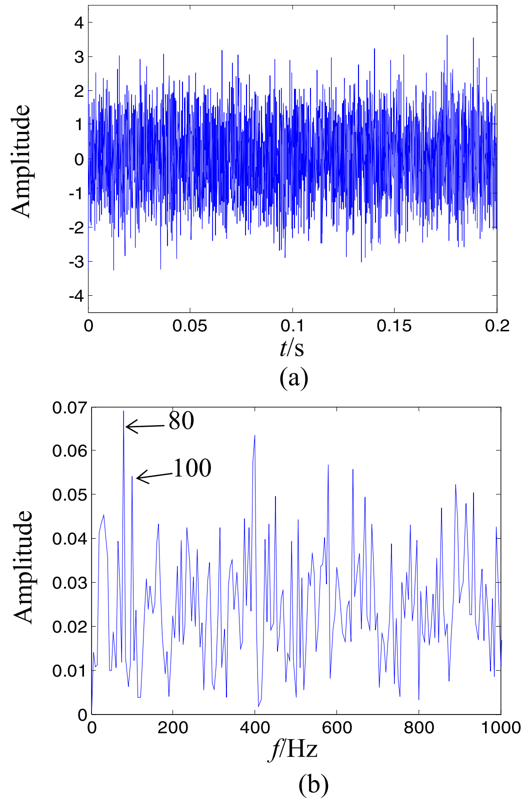

FIGURE 3. The simulation signal and corresponding Hilbert envelope spectrum: (a) the simulation signal, (b) the Hilbert envelope spectrum.

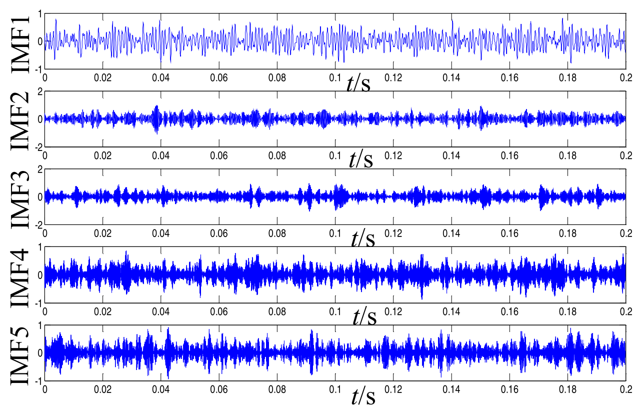

FIGURE 4. The decomposition result by VMD.

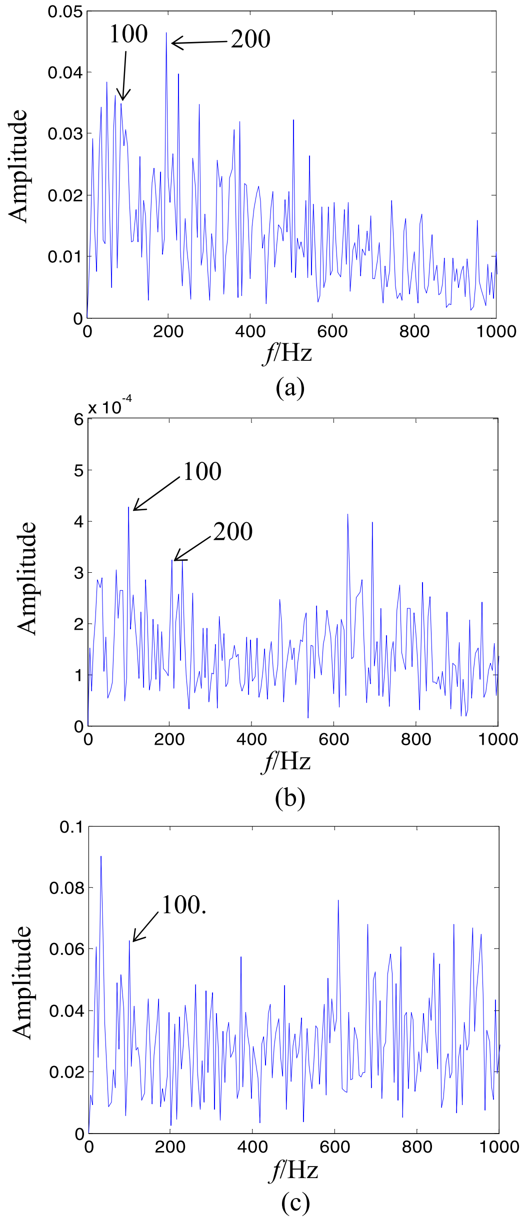

FIGURE 5. The Hilbert envelope spectra corresponding to: (a) the optimal IMF, (b) the enhance signal, (c) the simulation signal only using MED.

in which f_n and f_0 is the natural frequency of bearing, the rotating frequency of shafts, respectively, P is the amplitude coefficient, and S is the attenuation coefficient which can be defined as:

$$S = 2\pi f_n \gamma \tag{17}$$

where γ is the damping ratio.

In the simulation, the parameters are supposed as: $f_n = 4000Hz, f_0 = 30Hz, P = 0.01, T = 0.01s, \omega = 0.019894, S = 500, n(t)$ is a standard normal distribution with standard deviation 3, the sampling frequency $f_s = 20480Hz$ and the sampling points $N = 4096$.

Figs.3 (a) and (b) show the time domain waveform and Hilbert envelope spectrum of the simulation signal, respectively. As shown in Fig.3 (a), the periodic impulses are submerged due to the interference of the heavy noise. From Fig.3 (b), the faulty feature frequency ($100Hz$) is extracted roughly and submerged by unknown frequencies, such as $80Hz$ etc. The decomposition result using VMD is shows in Fig.4. In order to select the optimal IMF to track the faulty information, L-Kurtosis is introduced and the L-Kurtosis value corresponding to each IMF is shown in Table 1. From Table 1, we can see that the maximum L-Kurtosis value

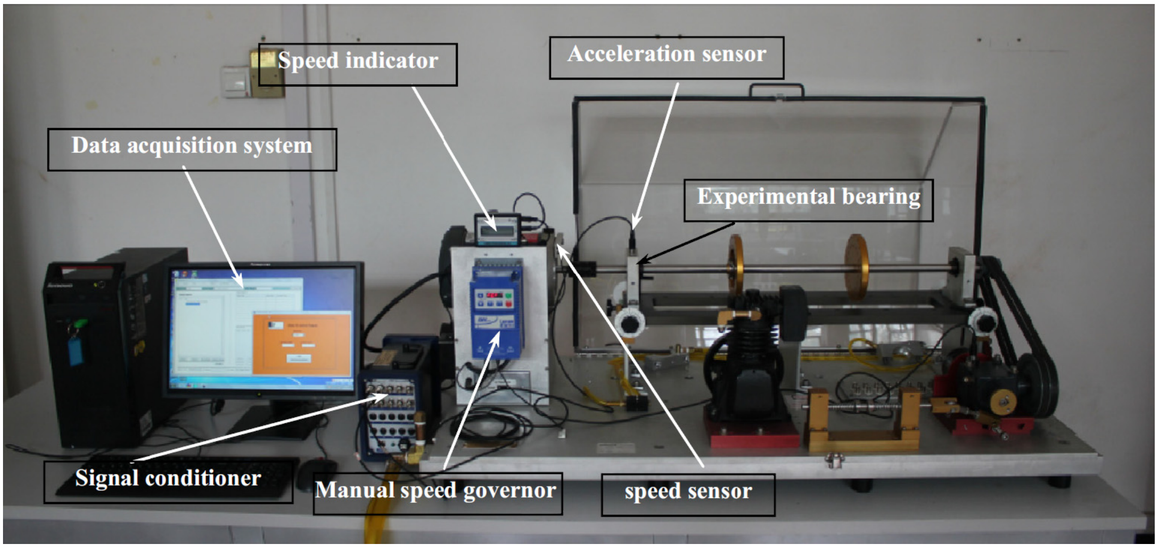

FIGURE 6. The machinery fault simulator test rig.

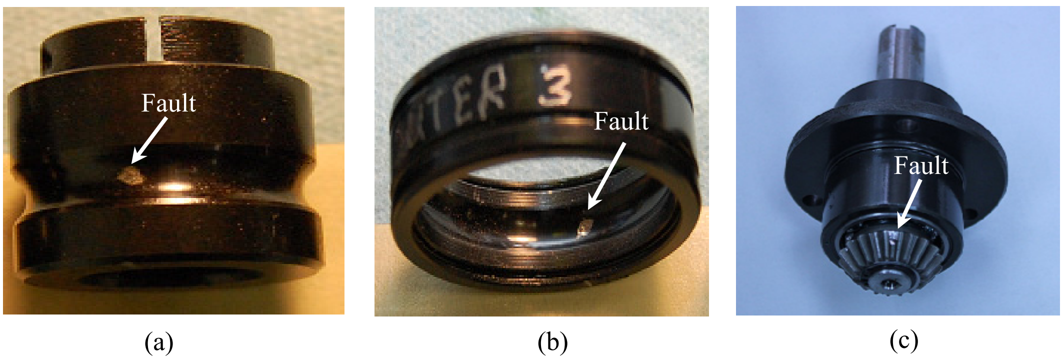

FIGURE 7. The faulty components: (a) the bearing with inner race fault, (b) the bearing with outer race fault, (c) the gear with a broken tooth.

corresponds to IMF3 and the Hilbert envelope spectrum of IMF3 is shown in Fig.5 (a). From Fig.5 (a), we can see that faulty feature frequency (100Hz) and its second harmonic (200Hz) are roughly extracted but still submerged by other frequencies. Therefore, MED is further employed to IMF3 to enhance the impact characteristic and the Hilbert envelope spectrum of the enhance signal is shown in Fig.5 (b). Fig.5 (c) shows the result of only using MED to the raw vibration signal. By comparing Figs.5 (a), (b) and (c), we can see that the faulty feature frequency (100Hz) and its second harmonic (200Hz) are more clearly extracted in Fig.5 (b). Based on the above analysis, the fault is detected successfully and the performance of the proposed strategy is verified. Meanwhile, the necessity of the combination of VMD, L-Kurtosis and MED is further indicated.

V. EXPERIMENTAL VERIFICATION

In this section, experimental vibration signals collected from the bearings with inner race fault, outer race fault and a gear with a broken tooth are used to verify the effectiveness of the proposed strategy.

TABLE 1. Details of the L-Kurtosis values corresponding to each IMF.

IMFs	IMF1	IMF2	IMF3	IMF4	IMF5
Kurtosis value	1.6424	3.1237	3.8177	2.8242	3.1386

Vibration measurements are conducted using the machinery fault simulator test rig [33] which is shown in Fig.6, and the experimental setup includes speed monitor, manual speed governor, acceleration sensors, speed sensors, motors, spindles and computer with VQ data acquisition software. The sampling frequency f_s is 25.6kHz.

The rolling bearings with the product type ER-12K and bevel gear are used in the experiment. The faults of inner race, outer race and broken tooth are the single pitting defections processed by electro-discharge machining, which are shown in Figs.7 (a), (b) and (c), respectively.

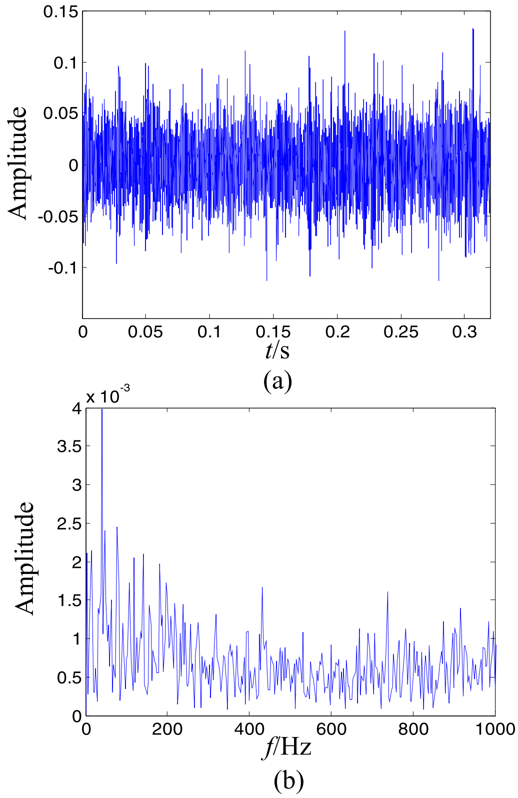

FIGURE 8. The raw signal and corresponding Hilbert envelope spectrum: (a) the raw signal, (b) the Hilbert envelope spectrum.

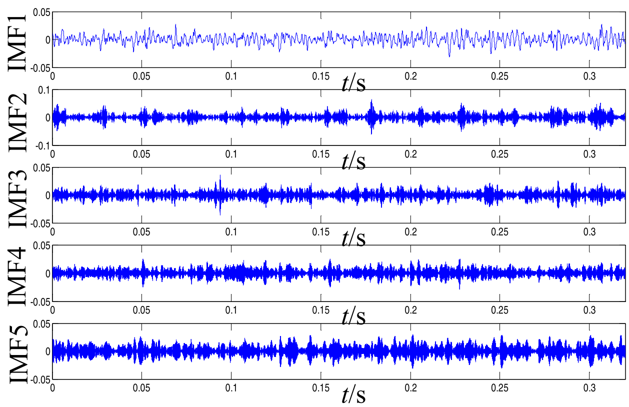

FIGURE 9. The decomposition result by VMD.

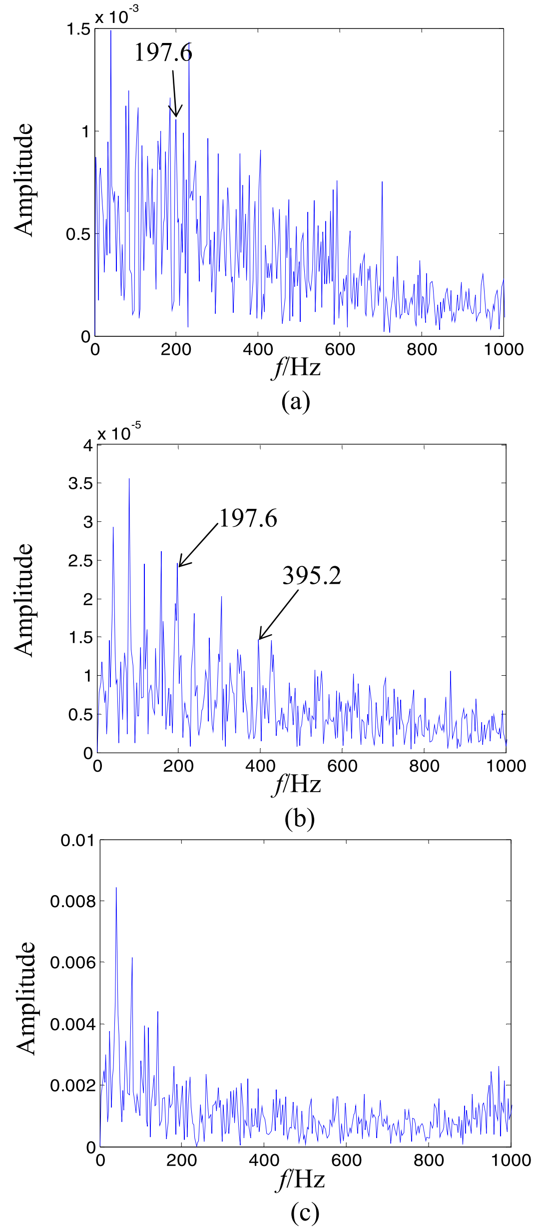

FIGURE 10. The Hilbert envelope spectrum corresponding to: (a) the optimal IMF, (b) the enhanced signal, (c) the raw signal only using VMD.

The parameters of the bearing are as follows: the number of rolling elements $N_b = 8$, ball diameter $B_d = 0.3125 inch$, pitch diameter $P_d = 1.318 inch$, the contact angle $\alpha = 0°$. For the bearing with inner race fault, the signal length is 8192 points and the shaft rotating frequency $f_{shaft} = 39.84Hz$. Hence, the ball pass frequency of inner race (BPFI) is [33]:

$$BPFI = \frac{N_b}{2} f_{shaft}\left(1 + \frac{B_d}{P_d}\cos\alpha\right) = 4.9484 f_{shaft} = 197.1Hz \tag{18}$$

For the bearing with outer race fault, the signal length is 8192 points and the shaft rotating frequency $f_{shaft} = 36.86Hz$. Hence, the ball pass frequency of the outer race (BPFO) is [33]:

$$BPFO = \frac{N_b}{2} f_{shaft}(1 - \frac{B_d}{P_d})\cos\alpha = 3.0516 f_{shaft} = 112.5Hz \tag{19}$$

For the gear with a broken tooth, the signal length is 8192 points, the shaft rotating frequency $f_{shaft} = 29.63Hz$ and the gear teeth $z = 18$. Different from bearing, the faulty feature frequencies of the gear with a broken tooth are the shaft rotating frequency and its harmonics [32], [34]. The gear mesh frequency f_m is equal to the product of the number of

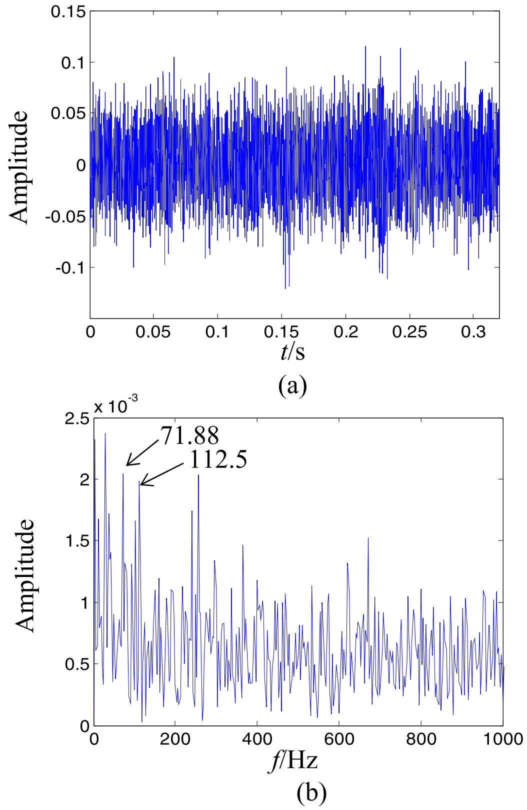

FIGURE 11. The raw signal and corresponding Hilbert envelope spectrum: (a) the raw signal, (b) the Hilbert envelope spectrum.

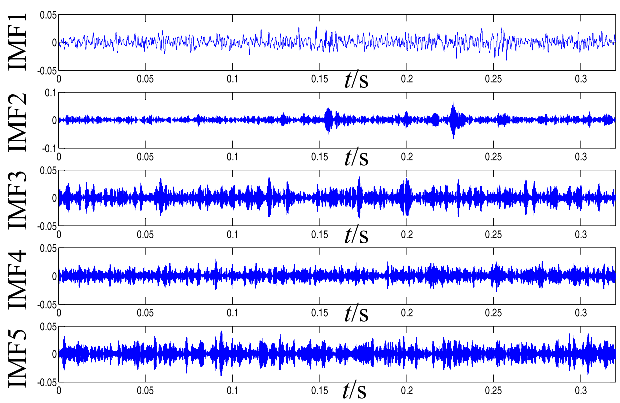

FIGURE 12. The decomposition result by VMD.

gear teeth and the shaft rotating frequency as:

$$f_m = z \times f_{shaft} = 18 \times 29.63 = 533.34Hz \tag{20}$$

A. INNER RACE FAULT DETECTION

The raw signal with inner race fault and its Hilbert envelope spectrum are shown in Figs.8 (a) and (b), respectively. From Fig.8, the periodic response signal and the faulty feature frequency cannot be seen. Therefore, the proposed strategy is applied.

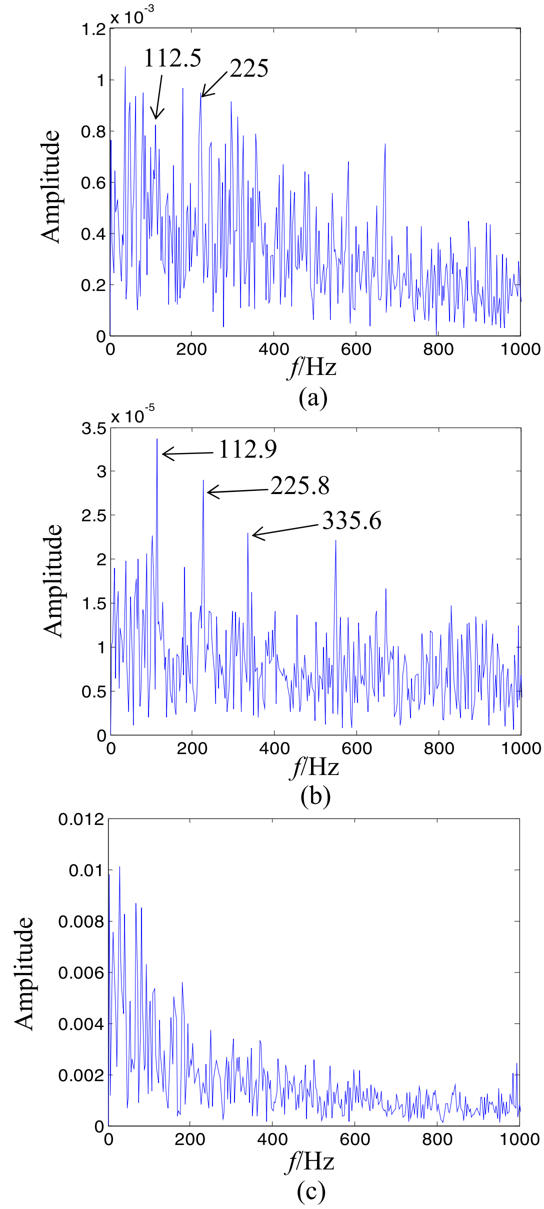

FIGURE 13. The Hilbert envelope spectrum corresponding to: (a) the optimal IMF, (b) the enhanced signal, (c) the raw signal only using VMD.

TABLE 2. Details of the L-kurtosis values corresponding to each IMF.

IMFs	IMF1	IMF2	IMF3	IMF4	IMF5
Kurtosis value	3.3158	3.4683	3.8723	3.4402	3.0653

VMD is used to the raw signal and the decomposition result is shown in Fig.9. Then, L-Kurtosis is used to each IMF and the corresponding L-Kurtosis value is shown in Table 2. As shown in Table 2, the maximum L-Kurtosis value corresponds to IMF3 and its Hilbert envelope spectrum is shown in Fig.10 (a). From Fig.10 (a), we can see that the faulty feature frequency (197.6Hz) is heavily submerged by numerous unknown frequency components. In order to extract fault

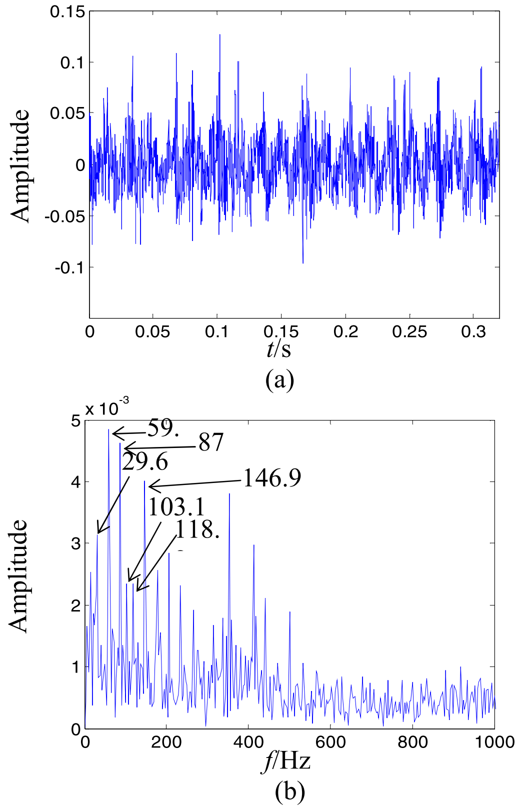

FIGURE 14. The raw signal and corresponding Hilbert envelope spectrum: (a) the raw signal, (b) the Hilbert envelope spectrum.

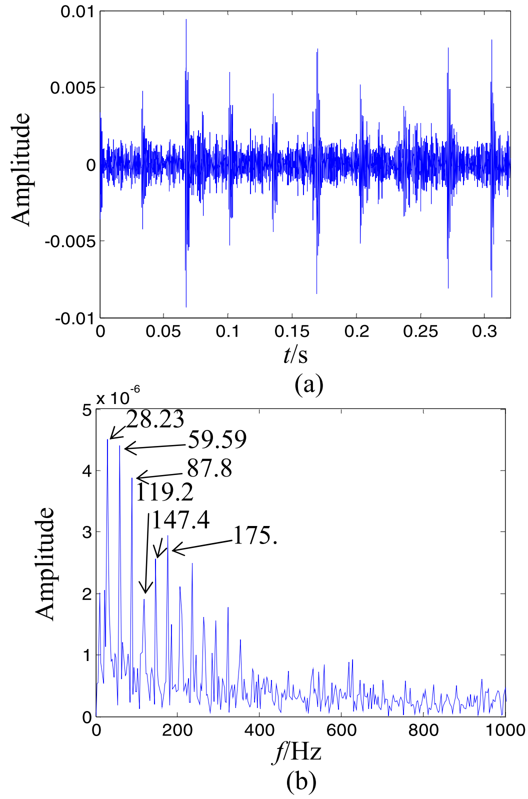

FIGURE 15. The enhanced signal and corresponding Hilbert envelope spectrum: (a) the enhanced signal, (b) the Hilbert envelope spectrum.

feature frequency, MED is further employed to IMF3 and the Hilbert envelope spectrum of the enhanced signal is shown in Fig.10 (b). As shown in Fig.10 (b), the faulty feature frequency (197.6Hz) and its second harmonic (395.2Hz) are accurately extracted, which are matched with the theoretical calculation value 197.1Hz (show in Eq.(18)) and its harmonic 394.2 Hz. Therefore, the bearing with inner race fault is definitely detected and the performance of the proposed strategy is verified.

To verify the necessity of the combination of three methods, the results of only using MED to the raw signal is given in Fig.10 (c). From Fig.10 (c), we can see that the faulty feature frequency cannot be extracted effectively.

B. OUTER RACE FAULT DETECTION

The raw signal with outer race fault and its Hilbert envelope spectrum are shown in Figs.11 (a) and (b), respectively. From Fig.11 (b), the faulty feature frequency (112.5Hz) is submerged by other frequency, such as 71.88Hz etc. The fault cannot be detected and the proposed strategy is applied.

Fig.12 and Table 3 show the decomposition result using VMD and the detailed L-Kurtosis value of each IMF, respectively. From Table 3, we can see that the optimal IMF is IMF4 which corresponds to the maximum L-Kurtosis value. The Hilbert envelope analysis is employed to IMF4 and the result is shown in Fig.13 (a). As shown in Fig.13 (a), the faulty feature frequency (112.5Hz) is hidden in numerous unknown frequency components.

TABLE 3. Details of the L-Kurtosis values corresponding to each IMF.

IMFs	IMF1	IMF2	IMF3	IMF4	IMF5
Kurtosis value	3.4511	2.9932	3.8135	7.5704	3.1085

In order to make the faulty feature frequency more prominent, MED is further used. Fig.13 (b) shows the Hilbert envelope spectrum of the enhanced signal, we can see that the faulty feature frequency (112.9Hz) and its 2 to 3 harmonics (225.8Hz, 335.6Hz) are clearly extracted. By matching the theoretical values 112.5Hz (show in Eq.(19)), the outer race fault is successfully detected. The performance of the proposed strategy is verified.

Meanwhile, the result of only using MED to the raw signal is given in Fig.13 (c). As shown in Fig.13 (c), the faulty feature frequency and its harmonics cannot be extracted effectively. Hence, the necessity of the combination of three methods is further confirmed.

C. BROKEN TEETH FAULT DETECTION

The raw signal with broken tooth fault and its Hilbert envelope spectrum are shown in Figs.14 (a) and (b), respectively. The next procedures are the same as the part 4.2.1 and

TABLE 4. Details of the L-Kurtosis values corresponding to each IMF.

IMFs	IMF1	IMF2	IMF3	IMF4	IMF5
Kurtosis value	2.5400	6.1686	5.1376	5.6178	12.7849

4.2.2. Table 4 shows the detailed L-Kurtosis value of each decomposed IMF. Figs.15 (a) and (b) show the time domain waveform of the enhanced signal and its corresponding Hilbert envelope spectrum. By Comparing Fig.14 (a) and Fig.15 (a), we can see that the impact characteristic is clearer in the latter graphic. The performance of the proposed strategy is further verified by comparing Fig.14 (b) and Fig.15 (b). As shown in Fig.14 (b), the shafting frequency (29.63Hz) and its harmonics (59.3Hz, 87Hz, 146.9Hz) are shown clearly, but its forth harmonic (118.8Hz) is submerged by the other frequency (103.1Hz). As shown in Fig.15 (b), the shafting frequency (28.23Hz) and its 2 to 6 harmonics (59.59Hz, 87.82Hz, 119.2Hz, 147.4Hz, 175.6Hz) are all shown clearly. The gear mesh frequency (show in Eq.(20)) are not shown in both Fig.14 (b) and Fig.15 (b). Therefore, the teeth fault of the gear is successfully detected.

VI. CONCLUSION

This paper proposed a strategy using VMD, L-Kurtosis and MED to detect the faults of mechanical components and achieve good effects. VMD has the obvious advantage in decomposing the non-stationary signal. L-Kurtosis is suitable to select the optimal IMF to track the faulty information. MED is used to enhance the periodic impact characteristic to make the fault feature more obvious. The introduction of L-Kurtosis not only overcomes the difficulty of choosing the optimal IMF, but also combines the strong non-stationary vibration signal decomposition ability of VMD and periodic impact characteristic enhancement ability of MED.

The effectiveness of the proposed strategy is verified by the numerical simulation and experimental investigations. Meanwhile, the necessity of the combination of three methods is indicated through the comparison investigations.

REFERENCES

[1] Y. Zhang and R. B. Randall, "Rolling element bearing fault diagnosis based on the combination of genetic algorithms and fast kurtogram," *Mech. Syst. Signal Process.*, vol. 23, no. 5, pp. 1509–1517, Jul. 2009.

[2] J. Xiang, Y. Zhong, and H. Gao, "Rolling element bearing fault detection using PPCA and spectral kurtosis," *Measurement*, vol. 75, pp. 180–191, Nov. 2015.

[3] Z. Wang, W. Du, J. Wang, J. Zhou, X. Han, Z. Zhang, and L. Huang, "Research and application of improved adaptive MOMEDA fault diagnosis method," *Measurement*, vol. 140, pp. 63–75, Jul. 2019.

[4] X. Liang, M. J. Zuo, and Z. Feng, "Dynamic modeling of gearbox faults: A review," *Mech. Syst. Signal Process.*, vol. 98, pp. 852–876, Jan. 2018.

[5] Z. Wang, G. He, W. Du, J. Zhou, X. Han, J. Wang, H. He, X. Guo, J. Wang, and Y. Kou, "Application of parameter optimized variational mode decomposition method in fault diagnosis of gearbox," *IEEE Access.*, vol. 7, pp. 44871–44882, 2019.

[6] F. Auger and P. Flandrin, "Improving the readability of time-frequency and time-scale representations by the reassignment method," *IEEE Trans. Signal Process.*, vol. 43, no. 5, pp. 1068–1089, May 1995.

[7] I. Djurović and L. Stanković, "Time–frequency representation based on the reassigned S-method," *Signal Process.*, vol. 77, no. 1, pp. 115–120, Aug. 1999.

[8] D. Klionskiy, M. Kupriyanov, and D. Kaplun, "Signal denoising based on empirical mode decomposition," *J. Vibroeng.*, vol. 19, no. 7, pp. 5560–5570, Nov. 2017.

[9] Z. Haiyang, W. Jindong, J. Lee, and L. Ying, "A compound interpolation envelope local mean decomposition and its application for fault diagnosis of reciprocating compressors," *Mech. Syst. Signal Process.*, vol. 110, pp. 273–295, Sep. 2018.

[10] F.-P. An, "Image feature extraction algorithm based on bi-dimensional local mean decomposition," *Opt. Rev.*, vol. 26, no. 1, pp. 43–64, Feb. 2019.

[11] J. Yu and J. Lv, "Weak fault feature extraction of rolling bearings using local mean decomposition-based multilayer hybrid denoising," *IEEE Trans. Instrum. Meas.*, vol. 66, no. 12, pp. 3148–3159, Dec. 2017.

[12] J. Cai, "Feature extraction of rolling bearing fault signal based on local mean decomposition and teager energy operator," *Ind. Lubrication Tribology*, vol. 69, no. 6, pp. 872–880, 2017.

[13] H. Liu and J. Xiang, "Kernel regression residual signal-based improved intrinsic time-scale decomposition for mechanical fault detection," *Meas. Sci. Technol.*, vol. 30, no. 1, Jan. 2019, Art. no. 015107.

[14] A. Hu, L. Xiang, and N. Gao, "Fault diagnosis for the gearbox of wind turbine combining ensemble intrinsic time-scale decomposition with Wigner bi-spectrum entropy," *J. Vibroeng.*, vol. 19, no. 3, pp. 1759–1770, May 2017.

[15] K. Dragomiretskiy and D. Zosso, "Variational mode decomposition," *IEEE Trans. Signal Process.*, vol. 62, no. 3, pp. 531–544, Feb. 2014.

[16] Y. Wang, R. Markert, J. Xiang, and W. Zheng, "Research on variational mode decomposition and its application in detecting rub-impact fault of the rotor system," *Mech. Syst. Signal Process.*, vols. 60–61, pp. 243–251, Aug. 2015.

[17] A. A. Abdoos, P. K. Mianaei, and M. R. Ghadikolaei, "Combined VMD-SVM based feature selection method for classification of power quality events," *Appl. Soft Comput.*, vol. 38, pp. 637–646, Jan. 2016.

[18] Z. Li, J. Chen, Y. Zi, and J. Pan, "Independence-oriented VMD to identify fault feature for wheel set bearing fault diagnosis of high speed locomotive," *Mech. Syst. Signal Process.*, vol. 85, pp. 512–529, Feb. 2017.

[19] J. Yao, Y. Xiang, S. Qian, S. Wang, and S. Wu, "Noise source identification of diesel engine based on variational mode decomposition and robust independent component analysis," *Appl. Acoust.*, vol. 116, pp. 184–194, Jan. 2017.

[20] C. Yi, Y. Lv, and Z. Dang, "A fault diagnosis scheme for rolling bearing based on particle swarm optimization in variational mode decomposition," *Shock Vib.*, vol. 2016, May 2016, Art. no. 9372691.

[21] X. Yan, M. Jia, and L. Xiang, "Compound fault diagnosis of rotating machinery based on OVMD and a 1.5-dimension envelope spectrum," *Meas. Sci. Technol.*, vol. 27, no. 7, Jul. 2016, Art. no. 075002.

[22] S. Zhang, Y. Wang, S. He, and Z. Jiang, "Bearing fault diagnosis based on variational mode decomposition and total variation denoising," *Meas. Sci. Technol.*, vol. 27, no. 7, Jul. 2016, Art. no. 075101.

[23] D. Dyer and R. M. Stewart, "Detection of rolling element bearing damage by statistical vibration analysis," *J. Mech. Des.*, vol. 100, no. 2, pp. 229–235, Apr. 1978.

[24] A. Parey, M. El Badaoui, F. Guillet, and N. Tandon, "Dynamic modelling of spur gear pair and application of empirical mode decomposition-based statistical analysis for early detection of localized tooth defect," *J. Sound Vib.*, vol. 294, no. 3, pp. 547–561, Jun. 2006.

[25] X. Wang, V. Makis, and M. Yang, "A wavelet approach to fault diagnosis of a gearbox under varying load conditions," *J. Sound Vib.*, vol. 329, no. 9, pp. 1570–1585, Apr. 2010.

[26] S. Liu, S. Hou, K. He, and W. Yang, "L-Kurtosis and its application for fault detection of rolling element bearings," *Measurement*, vol. 116, pp. 523–532, Feb. 2018.

[27] J. Li, M. Li, and J. Zhang, "Rolling bearing fault diagnosis based on time-delayed feedback monostable stochastic resonance and adaptive minimum entropy deconvolution," *J. Sound Vib.*, vol. 401, pp. 139–151, Aug. 2017.

[28] H. Endo and R. B. Randall, "Application of a minimum entropy deconvolution filter to enhance autoregressive model based gear tooth fault detection technique," *Mech. Syst. Signal Process.*, vol. 21, no. 2, pp. 906–919, Feb. 2007.

[29] H. Liu, B. Song, H. Qin, and Z. Qiu, "An adaptive-ADMM algorithm with support and signal value detection for compressed sensing," *IEEE Signal Process. Lett.*, vol. 20, no. 4, pp. 315–318, Apr. 2013.
[30] D. He, X. Wang, S. Li, J. Lin, and M. Zhao, "Identification of multiple faults in rotating machinery based on minimum entropy deconvolution combined with spectral kurtosis," *Mech. Syst. Signal Process.*, vol. 81, pp. 235–249, Dec. 2016.
[31] N. Sawalhi, R. B. Randall, and H. Endo, "The enhancement of fault detection and diagnosis in rolling element bearings using minimum entropy deconvolution combined with spectral kurtosis," *Mech. Syst. Signal Process.*, vol. 21, no. 6, pp. 2616–2633, Aug. 2007.
[32] Z. Wang, J. Zhou, J. Wang, W. Du, J. Wang, X. Han, and G. He, "A novel fault diagnosis method of gearbox based on maximum kurtosis spectral entropy deconvolution," *IEEE Access*, vol. 7, pp. 29520–29532, 2019.
[33] H. Liu and J. Xiang, "Kernel regression residual decomposition-based synchroextracting transform to detect faults in mechanical systems," *ISA Trans.*, vol. 87, pp. 251–263, Apr. 2019.
[34] L. Cui, T. Yao, Y. Zhang, X. Gong, and C. Kang, "Application of pattern recognition in gear faults based on the matching pursuit of a characteristic waveform," *Measurement*, vol. 104, pp. 212–222, Jul. 2017.

HUI LIU received the B.S. degree in automation from Jiangsu University, China, in 2016. He is currently pursuing the master's degree in mechanical engineering with Wenzhou University. His research interest includes faults detection of mechanical systems.

JIAWEI XIANG received the B.S. degree in mechatronics from Hunan University, China, in 1997, the M.S. degree from Guangxi University, China, in 2003, and the Ph.D. from Xi'an Jiaotong University, China, in 2006. He is currently a Professor with the College of Mechanical and Electrical Engineering, Wenzhou University, China. His research interests are the health monitoring of mechanical systems using numerical simulation and signal processing techniques.